

Spin coherence in a two-dimensional electron gas with Rashba spin-orbit interaction

T. P. Pareek and P. Bruno

Max-Planck-Institut für Mikrostrukturphysik, Weinberg 2, D-06120 Halle, Germany

(Received 12 November 2001; revised manuscript received 14 February 2002; published 31 May 2002)

We study spin-relaxation phenomena in a two-dimensional electron gas in the presence of Rashba spin-orbit coupling. A tight-binding model including Rashba spin-orbit coupling is used to study spin relaxation and spin diffusion in a two-dimensional electron gas within Landauer-Büttiker formalism. It is shown that the spin-diffusion length is not independent of the mean free path as predicted by the motional narrowing effect. Further it is demonstrated that spin relaxation is anisotropic and can show a nonmonotonic dependence on Fermi energy due to nonparabolicity of the band.

DOI: 10.1103/PhysRevB.65.241305

PACS number(s): 72.25.Dc, 72.25.Mk

The emerging field of spintronics relies on the use of electron spins within semiconductors for the storage of coherence and its possible use for magnetoelectronic applications.¹ For this it is desirable to know how the spin relaxation occurs in semiconductors. One of the ways through which spin polarization can be lost is via spin-orbit coupling. Of particular interest is the Rashba spin-orbit² coupling (RSO), which exists in asymmetric heterostructures and can be controlled by an external gate voltage.^{3,4} For a two-dimensional electron gas (2DEG) lying in the xy plane the RSO interaction takes the form $H_R = \alpha(k_y\sigma_x - k_x\sigma_y) \equiv \vec{B}_R(\vec{k}) \cdot \vec{\sigma}$, where $\vec{\sigma} = (\sigma_x, \sigma_y, \sigma_z)$ denotes the Pauli spin matrices, α is the RSO coupling parameter, and $\vec{B}_R(\vec{k})$ is the Rashba field. The direction and magnitude of the Rashba field $\vec{B}_R(\vec{k})$ depend on the electron momentum \vec{k} . RSO coupling causes a slow spin dephasing by a mechanism known as D'yakonov-Perel',⁵ which is a continuous spin precession during electron free flights, contrary to the other spin-relaxation processes like the Elliot-Yafet⁶ and Bir-Aronov-Pikus mechanisms,⁷ which lead to instantaneous spin flips. When an electron propagates, its spin precesses around the direction of $\vec{B}_R(\vec{k})$. The length over which its spin precesses by an angle π is known as spin precession length and is related to α as $L_{sp} \approx \pi/\alpha$. Scattering from boundary or impurity changes the direction of the Rashba field $\vec{B}_R(\vec{k})$ which depends on the electron wave vector and causes the electron to precess around a new direction. Thus randomizing the precession process causes spin relaxation. The corresponding spin-relaxation time τ_ϕ is given by $\tau_\phi \approx 1/(\omega^2\tau_{el})$, where τ_{el} is elastic-scattering time.^{8,9} The corresponding spin-diffusion length is given as $L_{sd} = \sqrt{(\frac{1}{2})v_F^2\tau_{el}\tau_\phi} = L_{sp}$ which is independent of the mean free path (L_e). It is important to realize that although the disorder increases the spin-relaxation time (motional narrowing effect^{8,9}), this increase is exactly compensated by the reduction of the diffusion constant, leading to a spin-diffusion length that is essentially independent of the disorder. The two latter quantities are probed by different kinds of experiments, namely, in a time-resolved or spatially resolved experiment, respectively. We report numerical calculation on a square lattice of length L_x (direction of current flow) and width L_y along the transverse direction, which shows that spin-diffusion length is not independent of the mean free

path (L_e) as predicted by the motional narrowing effect.⁸ We show that this deviation occurs in two opposite regimes, specifically, (i) the *diffusive* regime ($L_x \gg L_e, L_y \gg L_e$) when spin precession length is much larger than the mean free path ($L_{sp} \gg L_e$) and (ii) the *quasiballistic* regime ($L_x \gg L_e, L_y \ll L_e$) when spin precession length is much smaller than the mean free path ($L_{sp} \ll L_e$). Further it is shown that in case (i) where ($L_{sp} \gg L_e$), the spin-diffusion length can be nonmonotonic as a function of Fermi energy due to nonparabolicity of the band. It is also shown that spin relaxation is anisotropic which has important consequences for the Datta-Das transistor.¹⁰ These important results are reported in this paper. We would like to stress that the results presented here are obtained within the single band tight-binding model using a recursive Green-function method,¹¹ which is an exact method and takes into account the *quantum effects* at the single-particle level.

The Hamiltonian of a 2DEG lying in the xy plane in presence of Rashba spin-orbit coupling is in a continuum given by $H = \hbar^2(k_x^2 + k_y^2)/2m^* + \alpha(k_y\sigma_x - k_x\sigma_y) + V(x,y)$, where $V(x,y)$ is the confining potential. For $V(x,y)$ we choose a hard wall confining potential. We discretize the above Hamiltonian on a square lattice of lattice spacing a with N_x sites in the longitudinal direction (current direction) ($L_x = N_x a$) and N_y lattice sites along the transverse direction ($L_y = N_y a$), attached to two ideal nonmagnetic leads on the left and right. The corresponding tight-binding Hamiltonian, including the RSO,² takes the form^{11,12}

$$\begin{aligned}
 H = & \sum_{i,j,\sigma} \varepsilon c_{i,j,\sigma}^\dagger c_{i,j,\sigma} + t \sum_{\langle i,j \rangle \sigma} c_{i+1,j,\sigma}^\dagger c_{i,j,\sigma} + c_{i,j+1,\sigma}^\dagger c_{i,j,\sigma} \\
 & + \text{H.c.} - \lambda_{so} \sum_{i,j,\sigma,\sigma'} \{ -c_{i+1,j,\sigma}^\dagger c_{i,j,\sigma'} (i\sigma_y)^{\sigma\sigma'} \\
 & + c_{i,j+1,\sigma}^\dagger c_{i,j,\sigma'} (i\sigma_x)^{\sigma\sigma'} \} + \text{H.c.} \}. \quad (1)
 \end{aligned}$$

Here $c_{i,j,\sigma}^\dagger$ is the creation operator of an electron with spin σ at site (i,j) , ε is a random on-site energy (we use the random Anderson model for disorder with width W), t is the hopping energy ($t = \hbar^2/2m^*a^2$; we set $t=1$ for numerical simulation), $\sigma_x^{\sigma\sigma'}$, $\sigma_y^{\sigma\sigma'}$, and $\sigma_z^{\sigma\sigma'}$ are the Pauli matrix elements, the summation $\langle i,j \rangle$ runs over nearest-neighbor sites, and $\lambda_{so} = (\alpha/2a)$ is the RSO coupling parameter having a

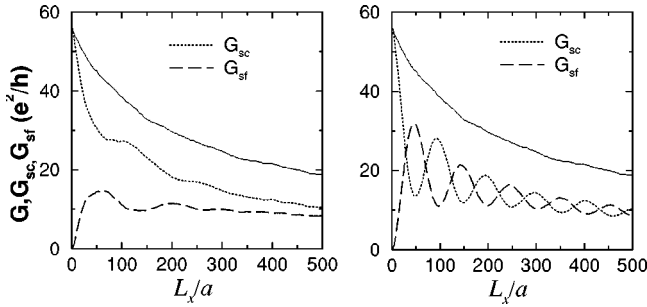


FIG. 1. Conductance (solid line), spin-conserved conductance (dashed line), and spin-flip conductance (dot-dashed line) as a function of channel length. The spin-quantization axis is along y for the left panel and along x axis for the right panel. The model parameters are $E_f = 1.1t$, $L_y = 80a$, $W = 0.5|t|$, and $\lambda_{so} = 0.03|t|$.

dimension of energy. The RSO coupling causes spin splitting for $\vec{k} \neq 0$, $\Delta E = 2\alpha k$, which is linear in momentum and at the same time causes the spin to precess around the Rashba field $\vec{B}_R(\vec{k})$ with frequency $\omega = \Delta E/2\hbar$.

For later reference we remind the reader that within the Born approximation the mean free path in two dimensions is given by $L_e = (12\hbar v_f/2\pi N_{2d}(E_f)W^2)a$, W is strength of the Anderson disorder, and $N_{2d}(E_f)$ is the density of states. Here we also remind that in two dimensions the density of states is singular in the middle of the band, while it goes to a constant near the band edge. We will see later that this can lead to a nonmonotonic behavior for spin-diffusion length as a function of Fermi energy.

The conductance and spin-resolved conductances are calculated using Landauer-Büttiker¹³ formalism with the help of nonequilibrium Green's-function formalism.¹¹ The two-terminal spin-resolved conductance (for a given spin-quantization axis) is given by¹¹ $G^{\sigma\sigma'}(\epsilon_F) = e^2/h \text{Tr}[\Gamma_1^\sigma G_{1N_x}^{\sigma\sigma'} + \Gamma_{N_x}^{\sigma'} G_{N_x 1}^{\sigma'\sigma}]$, where $\Gamma_{1(N_x)}$ is the self-energy function for the isolated ideal leads, which are given by $\Gamma_{p(q)} = t^2 A_{p(q)}$, where $A_{p(q)}$ is the spectral density in the respective lead when it is decoupled from the structure, and $G_{1N_x}^{\sigma\sigma'}$ and $G_{N_x 1}^{\sigma'\sigma}$ are the retarded and advanced Green's functions of the whole structure, taking leads into account. The trace is over spatial degrees of freedom. The total conductance is the sum of the spin-conserved conductance and spin-flip conductance, i.e., $G = G_{sc} + G_{sf}$, where the spin-conserved and spin-flip conductances are $G_{sc} = G^{\uparrow\uparrow} + G^{\downarrow\downarrow}$ and $G_{sf} = G^{\uparrow\downarrow} + G^{\downarrow\uparrow}$, respectively. We point out that in our simulation the injected current is unpolarized since the ideal leads are nonmagnetic, however by analyzing the spin-resolved conductances we can study the spin-relaxation and diffusion phenomena which would be observable when the injector and detector are magnetic. Note that it is also possible to obtain such information without magnetic leads, by polarizing and analyzing the electron gas optically.

Figure 1 depicts the conductance and spin-resolved conductance for different spin-quantization axes as a function of length L_x . The width of the channel is fixed and $L_y = 80a$. The other parameters are $L_e = 122a$ and $L_{sp} = 104a$. This set of parameters corresponds to the case (ii) discussed in the

introduction. The behavior of spin-resolved conductance is different for different quantization axes since the system considered here is confined along the transverse y direction, and the effective Rashba field $\vec{B}_R(\vec{k})$ is almost parallel to the y axis, hence the spin polarization does not show the oscillation when the spin-quantization axis is along y (left panel in Fig. 1). We note that the spin-diffusion length (L_{sd}) is larger than the spin precession length (L_{sp}). The right panel in Fig. 1 shows this clearly where G_{sc} and G_{sf} show oscillatory behavior as a function of length L_x , for lengths larger than the spin precession length ($L_{sp} = 104a$). The period of oscillation is given by L_{sp} and since there are many such oscillations it implies that L_{sd} is larger than the L_{sp} .¹⁴ In a recent model calculation by Silsbee¹⁵ no such oscillation was found. The model used in Ref. 15 ignores spin memory between successive scattering events, while our calculation is exact and hence the spin memory between successive scattering events is taken into account which is a *quantum effect*.

An appropriate quantity which is suitable to study spin diffusion is the polarization of the transmitted electrons, defined as $P = (G_{sc} - G_{sf})/(G_{sc} + G_{sf})$. From the definition it is clear that the polarization P lies strictly between $+1$ (spin conserved) and -1 (spin flip). The polarization corresponding to Fig. 1 is shown in Fig. 2. We see that the polarization is always positive for spin-quantization axis y while for spin-quantization axis z it shows oscillation of the largest amplitude. The amplitude of oscillation is different for different cases signifying that the spin-diffusion length is anisotropic.¹¹ This implies that for the Datta-Das¹⁰ spin transistor a larger current modulation will be obtained as a function of gate voltage when the magnetization direction of injector-detector ferromagnets is parallel to the z axis.¹⁶

Figure 3 illustrates the point that to preserve spin polarization one needs to confine electrons to a width of the order of the mean free path and not to tens of the mean free path as claimed from real-space Monte Carlo simulation.¹⁷ The mean free path (L_e) for Fig. 3 is $30a$; we see that the polarization for channel widths (L_y) $30a$, $50a$, and $80a$ decays much faster as a function of channel length compared to the channel widths $10a$, and $20a$, which are less than the mean free path. This corresponds to the quasiballistic case, i.e., the case (ii) discussed in the introduction. Also the polarization remains almost unchanged corresponding to channel width $10a$, which is consistent with the one-dimensional limit exhibiting no spin depolarization, since all rotations are along one axis and are commuting.¹⁸

Now we present the result for the regime (i) discussed in the introduction where $L_{sp} \gg L_e$ so that during free flight electron polarization precesses by an angle smaller than π . The results are shown in Fig. 4, where we have plotted polarization for spin-quantization axis y for different mean free paths as a function of spin precession length L_{sp} .

We see in Fig. 4 (left panel) that as we reduce the mean free path while keeping the spin precession length fixed we observe an enhancement of the polarization P , or in other words polarization decay is reduced, i.e., disorder helps to preserve spin polarization. For $\lambda_{so}/t \geq 0.02$, in the *quasiballistic* regime, polarization is enhanced as we increase λ_{so}/t

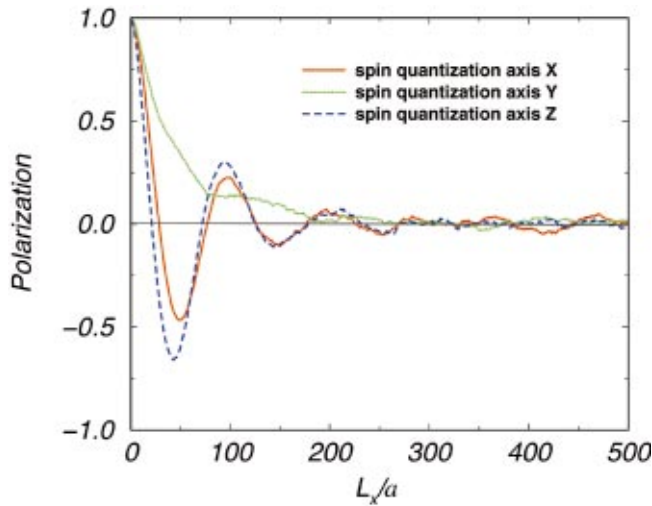


FIG. 2. (Color) Polarization as function of channel length for spin-quantization axes x , y , and z . The model parameters are the same as those for Fig. 1.

as is seen from the Fig. 4 right panel (curve corresponding to $L_e = 120a$). This corresponds to the case (ii) ($L_{sp}/L_e \ll 1$) discussed in the introduction, though the conditions are opposite to that of case (i) which is a motional narrowing regime. Hence in the diffusive case spin polarization is enhanced as we increase the dimensional parameter $L_{sp}/L_e \gg 1$ (Fig. 4, left panel) while for the quasiballistic case spin polarization is enhanced when $L_{sp}/L_e \ll 1$ (Fig. 4, right panel). In this sense these two opposite regimes behave similarly.

Thus encouraged by the results we study the spin diffusion as a function of Fermi energy. A motivation comes from the simple observation that the mean free path in two dimensions behaves like $L_e \approx \sqrt{(E_f)/[N_{2d}(E_f)W^2]}$; any deviation

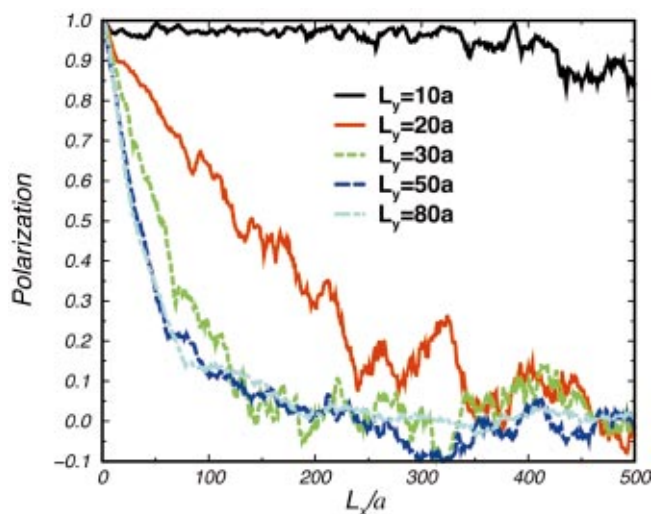


FIG. 3. (Color) Polarization as function of channel length for different channel widths. The mean free path and spin precession length are $30a$ and $104a$ ($\lambda_{so} = 0.03|t|$), respectively. The other parameters are the same as those for Fig. 1.

from nonparabolicity in the band will effect the density of states and therefore the spin relaxation. Near the band edges, where the energy band can be well approximated by parabola, the mean free path increases as Fermi energy is increased since $N_{2d}(E_f)$ is constant, however, as one approaches the band center $N_{2d}(E_f)$ starts to diverge logarithmically (Van Hove singularity); this in turn causes the mean free path to decrease. This is due to nonparabolicity of the energy band and in recent experiments by Hu *et al.*,⁴ it was reported to cause a reduction in the RSO coupling λ_{so} by 25%. The reduction in λ_{so} due to nonparabolicity is encouraging since it will increase the spin precession length which can only help to push the parameters in the regime (ii) discussed in the introduction. From the discussion above we

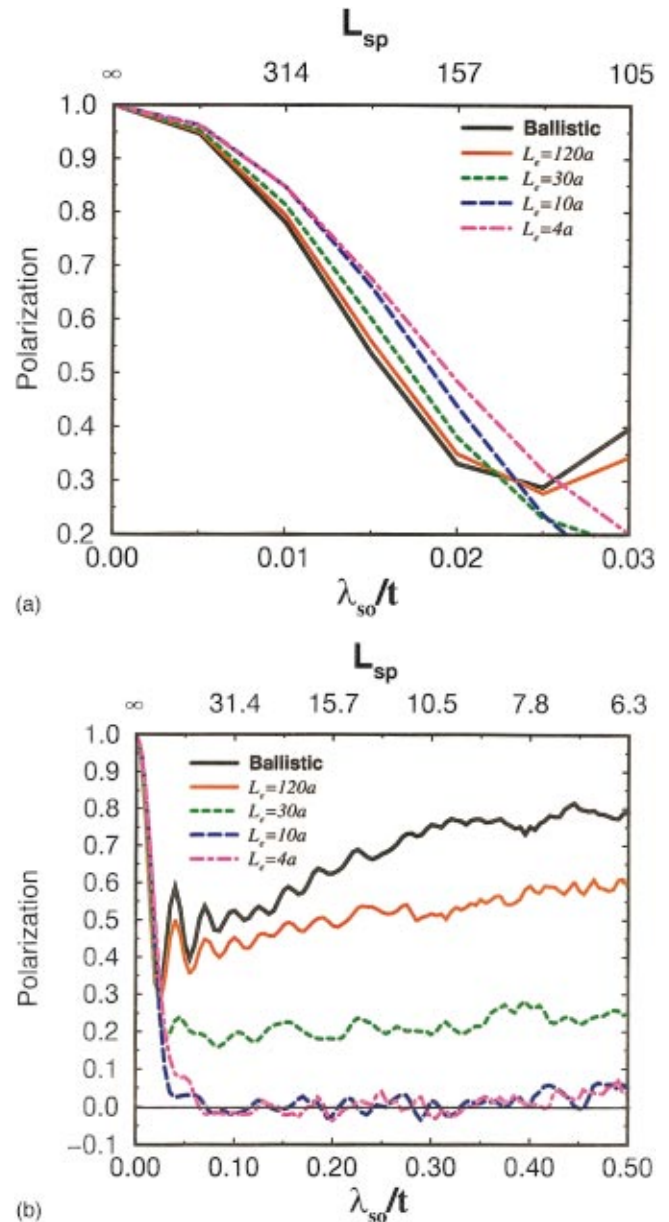


FIG. 4. (Color) Polarization as function of the RSO coupling parameter. Different curves correspond to different mean free paths as indicated in the figure. The length L_x and width L_y are both equal to $80a$ and $E_F = 1.1|t|$.

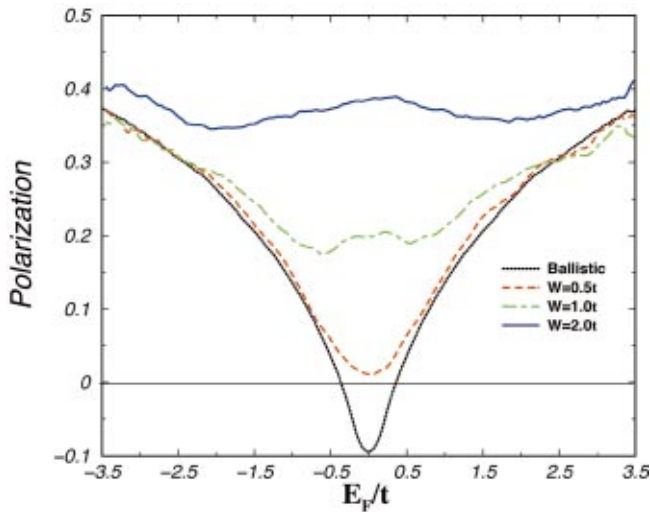


FIG. 5. (Color) Polarization as function of Fermi energy in units of $|t|$. Different curves correspond to different values of disorder strength W . The system size is $(80a \times 80a)$. The RSO coupling $\lambda_{so}/t=0.02$ ($L_{sp}=157a$). Disorder averaging was performed for 20 different realizations for each W .

see that as we move away from the band edges, initially the mean free path will increase and then start to decrease, and will be shortest at the band center. Though the presence of disorder will weaken the singularity in the density of states, the density of states still remains peaked at the band center as reported recently in Ref. 19. Hence enhancement of spin coherence, i.e., polarization, should be maximum at the band center. This is clearly seen in Fig. 5, where we have plotted polarization as a function of Fermi energy for different strengths of disorder, where $\lambda_{so}/t=0.02$ or the equivalent spin precession length is $L_{sp}=157a$. We notice that in the

middle of the band, polarization enhancement is largest compared to the ballistic case even for the weak disorder, i.e., $W/t=0.5$ and 1.0 . This is in agreement with the fact that densities of states are peaked at the band center.¹⁹

In the energy window $-2 \leq E_f/t \leq 2$ we are always in the regime of infinitesimal rotations, i.e., $L_{sp}/L_e \gg 1$, hence polarization is enhanced compared to the ballistic case irrespective of disorder strength. Beyond $-2 \leq E_f/t \leq 0$ the curve for $W/t=2.0$ shows an increase in polarization. This is expected since an increase in disorder only helps to decrease the mean free path. This is in agreement with heuristic arguments presented above. So from this curve we can safely draw the conclusion that as we move away from the band edge, polarization will decrease initially and then will start to increase again it reaches the band center, i.e., polarization shows a nonmonotonic behavior as a function of Fermi energy. This nonmonotonic behavior should be seen with reference to recent experiments on n -type GaAs,²⁰ where the observed spin lifetime shows a nonmonotonic behavior as a function of carrier density. In this experiment carrier density was controlled through doping, which increases the Fermi energy and reduces the mean free path. However the results of Ref. 20 are for three-dimensional bulk material, hence we cannot make a direct comparison with the experimental result. Another interesting conclusion which can be drawn from Fig. 5 is that in the diffusive case spin polarization can be preserved even for wide channels. This is clearly illustrated in Fig. 5 where all the curves in the presence of disorder lie above the curve for the ballistic case in the range $-2 \leq E_f/t \leq 2$. This might have an important implication for the Datta-Das spin transistor,¹⁰ since it removes the stringent criterion to confine electrons in one dimension.

This work was financially supported by the German Federal Ministry of Research (BMBF).

¹G. Prinz, Phys. Today **48**, 58 (1995).

²Yu.A. Bychkov and E.I. Rashba, Zh. Éksp. Teor. Fiz. **39**, 66 (1984) [Sov. Phys. JETP **39**, 78 (1984)].

³G. Lommer *et al.*, Phys. Rev. Lett. **60**, 728 (1988); B. Das *et al.*, Phys. Rev. B **41**, 8278 (1990); J. Nitta *et al.*, Phys. Rev. Lett. **78**, 1335 (1997); J.P. Heida *et al.*, Phys. Rev. B **57**, 11 911 (1998); G. Engels *et al.*, *ibid.* **55**, 1958 (1997); T. Matsuyama *et al.*, *ibid.* **61**, 15 588 (2000).

⁴C.-M. Hu *et al.*, Phys. Rev. B **60**, 7736 (1999).

⁵M.I. D'yakonov and V.I. Perel', Zh. Éksp. Teor. Fiz. **60**, 1954 (1971) [Sov. Phys. JETP **33**, 1053 (1971)].

⁶R.J. Elliot, Phys. Rev. **96**, 266 (1954); Y. Yafet, in *Solid State Physics*, edited by F. Seitz and D. Turnbull (Academic, New York, 1963), Vol. 14.

⁷G.L. Bir, A.G. Aronov, and G.E. Pikus, Zh. Éksp. Teor. Fiz. **69**, 1389 (1975) [Sov. Phys. JETP **42**, 705 (1976)].

⁸C.P. Slichter, *Principles of Magnetic Resonance* (Harper & Row, New York, 1963); M.Z. Maialle *et al.*, Phys. Rev. B **47**, 15 776 (1993).

⁹G.L. Chen *et al.*, Phys. Rev. B **47**, 4084 (1993).

¹⁰S. Datta and B. Das, Appl. Phys. Lett. **56**, 665 (1990).

¹¹T.P. Pareek and P. Bruno, Phys. Rev. B **63**, 165424-1 (2001); P. Bruno and T.P. Pareek, cond-mat/0105506 (unpublished); L.W. Molenkamp, G. Schmidt, and G.E.W. Bauer, Phys. Rev. B **62**, R4790 (2000); T.P. Pareek, cond-mat/0110440 (unpublished).

¹²F. Mireles and G. Kirczenow, Phys. Rev. B **64**, 024426 (2001).

¹³M. Büttiker, Phys. Rev. Lett. **57**, 1761 (1986); IBM J. Res. Dev. **32**, 317 (1988).

¹⁴A.G. Mal'shukov and K.A. Chao, Phys. Rev. B **61**, R2413 (2000).

¹⁵R.H. Silsbee, Phys. Rev. B **63**, 155305 (2001).

¹⁶H.X. Tang *et al.*, Phys. Rev. B **61**, 4437 (2000).

¹⁷A.A. Kiselev and K.W. Kim, Phys. Rev. B **61**, 13 115 (2000).

¹⁸A. Bournel *et al.*, Eur. Phys. J.: Appl. Phys. **4**, 1 (1998); Physica B **4**, 272 (1999).

¹⁹Y. Avishai and Y. Mier, cond-mat/0107591 (unpublished).

²⁰J.M. Kikkawa *et al.*, Science **277**, 1284 (1997); J.M. Kikkawa and D.D. Awschalom, Phys. Rev. Lett. **80**, 4313 (1998).